Substance specific chemical sensing with pristine and modified photonic nanoarchitectures occurring in blue butterfly wing scales

Gábor Piszter,[1] Krisztián Kertész,[1,*] Zofia Vértesy,[1] Zsolt Bálint,[2] and László Péter Biró[1]

[1]*Institute of Technical Physics and Materials Science, Research Centre for Natural Sciences, 1525 Budapest, PO Box 49, Hungary*

[2]*Hungarian Natural History Museum, H-1088, Budapest, Baross utca 13, Hungary*

[*]*kertesz.krisztian@ttk.mta.hu*

http://www.nanotechnology.hu

Abstract: Butterfly wing scales containing photonic nanoarchitectures act as chemically selective sensors due to their color change when mixing vapors in the atmosphere. Based on butterfly vision, we built a model for efficient characterization of the spectral changes in different atmospheres. The spectral shift is vapor specific and proportional with the vapor concentration. Results were compared to standard principal component analysis. The modification of the chemical properties of the scale surface by the deposition of 5 nm of Al_2O_3 significantly alters the character of the optical response. This is proof of the possibility to purposefully tune the selectivity of such sensors.

OCIS codes: (230.5298) Photonic crystals; (160.1435) Biomaterials; (120.0280) Remote sensing and sensors; (330.5310) Vision - photoreceptors.

References and links

1. R. A. Potyrailo, H. Ghiradella, A. Vertiatchikh, K. Dovidenko, J. R. Cournoyer, and E. Olson, "Morpho butterfly wing scales demonstrate highly selective vapour response," Nat. Photon. **1**(2), 123–128 (2007).
2. O. Frazão, J. L. Santos, F. M. Araújo, and L. A. Ferreira, "Optical sensing with photonic crystal fibers," Laser Photon. Rev. **2**(6), 449–459 (2008).
3. R. A. Potyrailo and R. R. Naik, "Bionanomaterials and bioinspired nanostructures for selective vapor sensing," Annu. Rev. Mater. Res. **43**(1), 307–334 (2013).
4. K. Kertész, G. Piszter, E. Jakab, Z. Bálint, Z. Vértesy, and L. P. Biró, "Color change of Blue butterfly wing scales in an air – vapor ambient," Appl. Surf. Sci. **281**, 49–53 (2013).
5. J. D. Joannopoulos, R. Meade, and D. J. N. Winn, *Photonic Crystals: Molding the Flow of Light* (Princeton University, 1995).
6. L. P. Biró and J. P. Vigneron, "Photonic nanoarchitectures in butterflies and beetles: valuable sources for bioinspiration," Laser Photon. Rev. **5**(1), 27–51 (2011).
7. C. Pacholski, "Photonic crystal sensors based on porous silicon," Sensors **13**(4), 4694–4713 (2013).
8. R. V. Nair and R. Vijaya, "Photonic crystal sensors: an overview," Prog. Quantum Electron. **34**(3), 89–134 (2010).
9. J. Shin, P. V. Braun, and W. Lee, "Fast response photonic crystal pH sensor based on templated photo-polymerized hydrogel inverse opal," Sens. Actuators B Chem. **150**(1), 183–190 (2010).
10. L. P. Biró, K. Kertész, Z. Vértesy, and Z. Bálint, "Photonic nanoarchitectures occurring in butterfly scales as selective gas/vapor sensors," Proc. SPIE **7057**, 705706 (2008).
11. Z. Bálint, K. Kertész, G. Piszter, Z. Vértesy, and L. P. Biró, "The well-tuned Blues: the role of structural colours as optical signals in the species recognition of a local butterfly fauna (Lepidoptera: Lycaenidae: Polyommatinae)," J. R. Soc. Interface **9**(73), 1745–1756 (2012).
12. Z. Bálint, J. Wojtusiak, G. Piszter, K. Kertész, and L. P. Biró, "Spectroboard: an instrument for measuring spectral characteristics of butterfly wings – a new tool for taxonomists," Genus **21**, 1–6 (2010).
13. M. P. Sison-Mangus, A. D. Briscoe, G. Zaccardi, H. Knüttel, and A. Kelber, "The lycaenid butterfly *Polyommatus icarus* uses a duplicated blue opsin to see green," J. Exp. Biol. **211**(3), 361–369 (2008).
14. D. G. Stavenga and K. Arikawa, "Photoreceptor spectral sensitivities of the Small White butterfly *Pieris rapae crucivora* interpreted with optical modeling," J. Comp. Physiol. A Neuroethol. Sens. Neural Behav. Physiol. **197**(4), 373–385 (2011).
15. P.-J. Chen, K. Arikawa, and E.-C. Yang, "Diversity of the photoreceptors and spectral opponency in the compound eye of the Golden Birdwing, *Troides aeacus formosanus*," PLoS ONE **8**(4), e62240 (2013).

#220109 - $15.00 USD Received 30 Jul 2014; revised 28 Aug 2014; accepted 28 Aug 2014; published 11 Sep 2014

16. K. Kertész, G. Piszter, E. Jakab, Z. Bálint, Z. Vértesy, and L. P. Biró, "Selective optical gas sensors using butterfly wing scales nanostructures," Key Eng. Mater. **543**, 97–100 (2013).
17. L. P. Biró, Z. Bálint, K. Kertész, Z. Vértesy, G. Márk, Z. Horváth, J. Balázs, D. Méhn, I. Kiricsi, V. Lousse, and J. P. Vigneron, "Role of photonic-crystal-type structures in the thermal regulation of a Lycaenid butterfly sister species pair," Phys. Rev. E Stat. Nonlin. Soft Matter Phys. **67**(2), 021907 (2003).
18. K. Kertész, Z. Bálint, Z. Vértesy, G. Márk, V. Lousse, J. Vigneron, M. Rassart, and L. Biró, "Gleaming and dull surface textures from photonic-crystal-type nanostructures in the butterfly *Cyanophrys remus*," Phys. Rev. E Stat. Nonlin. Soft Matter Phys. **74**(2), 021922 (2006).
19. Y. Ohno, "CIE Fundamentals for color measurements," in *Int. Conf. on Digital Printing Technologies*, 15–20 October 2000, Vancouver, Canada (2000), pp. 540–545.
20. I. T. Jolliffe, *Principal Component Analysis*, 2nd ed. (Springer-Verlag, 2002).
21. G. Piszter, K. Kertész, Z. Vértesy, Z. Bálint, and L. P. Biró, "Color based discrimination of chitin–air nanocomposites in butterfly scales and their role in conspecific recognition," Anal. Methods **3**(1), 78–81 (2011).
22. S. Mouchet, O. Deparis, and J. P. Vigneron, "Unexplained high sensitivity of the reflectance of porous natural photonic structures to the presence of gases and vapours in the atmosphere," Proc. SPIE **8424**, 842425 (2012).
23. K. Kertész, G. Piszter, Z. Baji, E. Jakab, Z. Bálint, Z. Vértesy, and L. P. Biró, "Vapor sensing on bare and modified blue butterfly wing scales," Chem. Sensors **4**, 17 (2014).
24. Y. Ding, S. Xu, Y. Zhang, A. C. Wang, M. H. Wang, Y. Xiu, C. P. Wong, and Z. L. Wang, "Modifying the anti-wetting property of butterfly wings and water strider legs by atomic layer deposition coating: surface materials versus geometry," Nanotechnology **19**(35), 355708 (2008).
25. S. H. Tan, A. L. Ahmad, M. G. M. Nawawi, and H. Hassan, "Separation of aqueous isopropanol through chitosan/poly(vinylalcohol) blended membranes by prevaporation," IIUM Eng. J. **2**, 7–12 (2001).

1. Introduction

Nowadays, the potential applications of photonic crystal type materials in sensing [1] are in the focus of attention [2,3]. As sensors penetrate the everyday life, the vigorous development of sensorics tries to cover the need for miniature sensor systems which are capable of making distinction between vapors of different volatile organic compounds (VOCs) and have fast response time combined with low energy consumption [3]. Selective chemical sensors based on photonic nanoarchitectures, like those in the wing scales of butterflies possessing structural coloration [4] may offer cheap solution to this problem.

Photonic nanoarchitectures are nanocomposites which are capable of interacting in a spectrally selective way with white light [5]. For color generation in the visible, the periodicity of optical properties (refractive index) has to be in the range of few 100 nm. This condition is well fulfilled by several photonic nanoarchitectures of biologic origin [6]. Color change of such biologic nanoarchitectures may originate from two sources: change of the refractive index of one, or both of the two optically different materials (refractive index contrast is needed for the appearance of the photonic band gap [5]), or from the change of the characteristic dimensions of the elements building up the photonic nanocomposite. Fortunately, the butterfly wing scales possessing structural coloration are nanocomposites of chitin and air. This allows for their use as selective chemical sensors for volatile vapors present in the ambient atmosphere. Due to the fast development of the response signal and relatively easy optical readout of optical sensors, various materials and setups are under investigation for fast and chemically selective sensors [7–9]. Among the high variety of inorganic materials there are also promising biological or bioinspired materials for sensors [3,10].

Our recent investigations showed that in the case of nine closely related blue Polyommatus butterfly species the spectral sensitivity of their eyes (sensor) and the dorsal structural coloration of the wings (measured object) are well tuned for safe mate / competitor recognition [11]. Based on our noninvasive spectral measurements [12] on numerous museum exemplars, we showed that the dorsal coloration is species specific and stable in time. The species of the investigated exemplars can be distinguished based on the dorsal coloration even in the case of the three violet species appearing to the human eye as similarly colored [11,12]. This clearly shows that the eyes of these butterflies are well tuned for the detection of minor color differences between the species, and the enhanced spectral sensitivity of the eyes concentrates on the wavelength range corresponding to the structural coloration. The compound eyes of the butterflies in certain cases contain four [13] or more [14,15] photoreceptors which can improve the spectral sensitivity at shorter wavelengths. In the case

#220109 - $15.00 USD Received 30 Jul 2014; revised 28 Aug 2014; accepted 28 Aug 2014; published 11 Sep 2014

of blue Polyommatus butterflies there are four photoreceptors [13]: three of them are similar to the photoreceptors in the human eye but there is one additional in the near UV – blue wavelength region which allows better discrimination of the bluish colors.

Butterfly wing scales containing 3D photonic nanoarchitectures exhibit measurable color change when mixing in the ambient atmosphere different types of volatile vapors [1,10]. In the case of the Polyommatine butterflies investigated earlier [11], both the color differences between the species [11] and the color change caused by the vapors [4,16] originate from the alteration of the structural color in the same near UV – blue wavelength region and they are of similar magnitude. Earlier we showed [11] that minor color differences between the Polyommatine species dorsal side are originated from the slight structural differences of their photonic nanoarchitectures, all exhibiting the same general layout called "pepper-pot" type scales [17]. Similarly minor color changes of a butterfly wing could be caused by the changes of the surrounding vapor mixtures: the refractive index contrast changes between the empty (chitin – air) and filled (chitin – vapor and condensed vapor - due to capillary condensation in the nanovoids [4]) state of the structure. These two analogous behaviors suggests the use of tridimensional color space representation to monitor the changes caused by vapors, as it was used with success for the species discrimination [11].

2. Materials and methods

The investigated butterfly exemplars which were used as sensor material were obtained from the curated Lepidoptera collection of the Hungarian Natural History Museum. For scanning electron microscope (SEM) imaging usual sample preparation was carried out [18]: a 25 mm^2 wing piece was cut and fixed on stubs, then coated with 15 nm gold to prevent the charging artifacts. For vapor sensing measurements we used a home-built setup [16]. This contains a 9.75 cm^3 gas flow cell which is an air-proof aluminum box with a quartz window for the optical reflectance measurements. Through its gas inlet and outlet different concentrations of volatile vapors were passed. The required vapor concentration was set by mixing the saturated vapors obtained from gas bubblers containing the pure liquids (from VWR, reagent grade) with artificial air (Messer, 80% N_2, 20% O_2, others < 20 ppm). The mixing ratio was set by computer controlled digital mass flow controllers (Aalborg DFC) so as the total flow of the mixture was kept at 1000 ml/min. Optical reflectance spectra on the butterfly wing samples were measured through the quartz window of the gas flow cell with the use of Avantes HS 1024*122TEC spectrometer. Normal incidence illumination was used, while the reflected light was collected at about 45° of angle of detection adjusted to get the highest reflectance signal. To obtain the reflectance spectra for 10 to 100% vapor concentration values in 10% steps, the following process was used. By means of a dedicated Labview code the digital flow controllers were set to output a succession of pairs: 20 s mixture flow followed by 60 s of synthetic air flow, to purge the cell. Repeating these pairs with increasing vapor concentrations we were able to record characteristic spectra for each of the investigated substances. The 60 s purging time is required to recover the initial reflectance value before the introduction of the next vapor mixture. Using this measurement protocol high reflectance signals were obtained while the memory effects were negligible.

To evaluate the vapor sensing data we used the color representation of the Polyommatine butterflies based on the CIE tristimulus color matching [11,19]. This tridimensional color space was created using the sensitivity functions of the four photoreceptors occurring in the eyes of the Lycaenid butterflies [13]. Comparing it with the standard (human) chromaticity diagram (CIE 1931) which is two-dimensional we expect better discrimination of the vapor sensing reflectance signals due to the additional visual pigment in the blue – UV range. Computing the light stimuli in the four photoreceptors, the following quantities were used:

$\Phi_{(\lambda)}$ the spectral irradiance of the light source (in our case, the CIE D65 standard illuminant)

$R_{(\lambda)}$ the spectral reflectance of the surface under perception,

#220109 - $15.00 USD Received 30 Jul 2014; revised 28 Aug 2014; accepted 28 Aug 2014; published 11 Sep 2014

$u_{(\lambda)}, b_{(\lambda)}, g_{(\lambda)}, y_{(\lambda)}$ correspond to the CIE color-matching functions; here these represent the absorbance spectra of UV, blue, green and yellow visual pigments respectively, according to [13].

For the tristimulus calculations, the corresponding quantities are

$$\begin{aligned} X &= \int_{300nm}^{700nm} \Phi_{(\lambda)} R_{(\lambda)}\, \mathrm{u}_{(\lambda)}\, \mathrm{d}\lambda, \\ Y &= \int_{300nm}^{700nm} \Phi_{(\lambda)} R_{(\lambda)} b_{(\lambda)}\, \mathrm{d}\lambda, \\ Z &= \int_{300nm}^{700nm} \Phi_{(\lambda)} R_{(\lambda)} g_{(\lambda)}\, \mathrm{d}\lambda, \\ W &= \int_{300nm}^{700nm} \Phi_{(\lambda)} R_{(\lambda)} y_{(\lambda)}\, \mathrm{d}\lambda. \end{aligned} \tag{1}$$

With these four values (Eq. (1)) we can characterize the effect of an arbitrary reflectance in the butterfly eye. To visualize it in 3D, we can calculate the four chromaticity values (Eq. (2)) from which the first three can be plot using the normalization condition of w:

$$\begin{aligned} x &= \frac{X}{X+Y+Z+W}, \\ y &= \frac{Y}{X+Y+Z+W}, \\ z &= \frac{Z}{X+Y+Z+W}, \\ w &= \frac{W}{X+Y+Z+W} = 1 - \mathrm{x} - \mathrm{y} - \mathrm{z}. \end{aligned} \tag{2}$$

To complete the calculus, the measured wing surface reflectance after each concentration step of the investigated substance was used in the 300 – 700 nm range. Integration of D65 illuminant, pigment absorbance and wing reflectance was performed with 1 nm resolution.

Control evaluation of the data from the vapor sensing experiments was carried out using principal component analysis (PCA). PCA is a widespread pattern-recognition technique for multivariate signals. The basic idea of the PCA is to reduce the dimensionality of the data set consisting of a large number of interrelated variables, while retaining as much as possible of the variation present in the data set. This is achieved by transforming the initial set of variables to weighted sums, called the principal components (PCs), and ordered so that the first few retain most of the variation present in all of the original variables [20].

Based on the SEM and TEM (Figs. 1(c) and 1(d)) images the general layout of the photonic nanoarchitectures occurring in the wing scales of the nine Polyommatine species is very similar, they exhibit only slight species-specific variations in the structural characteristics [11]. In certain cases these variations generate only minor color differences between the species, but of sufficient magnitude for a safe species discrimination [11,21]. Using a proper artificial neural network analysis of the reflectance spectra [21] and the structural data based on the SEM and TEM images [11] the discrimination of the nine species is possible with more than 90% accuracy. Even if the butterfly individuals were collected from different places within Hungary and in different years, the structural and spectral characteristics are similar. For the practical application of butterfly wings as ready-made vapor sensors this property is essential to provide the constant high quality of the sensor material. In our recent work [16], we compared the optical sensing properties of the dorsal wing surfaces of the nine Polyommatine butter⟩y species using optical spectrophotometry, and the species with the highest relative spectral change, the Common Blue (Lycaenidae:

#220109 - $15.00 USD Received 30 Jul 2014; revised 28 Aug 2014; accepted 28 Aug 2014; published 11 Sep 2014

Polyommatinae: Polyommatini: Polyommatina: *Polyommatus icarus*) was selected for further experiments (see Figs. 1(a) and 1(b)).

3. Results and discussion

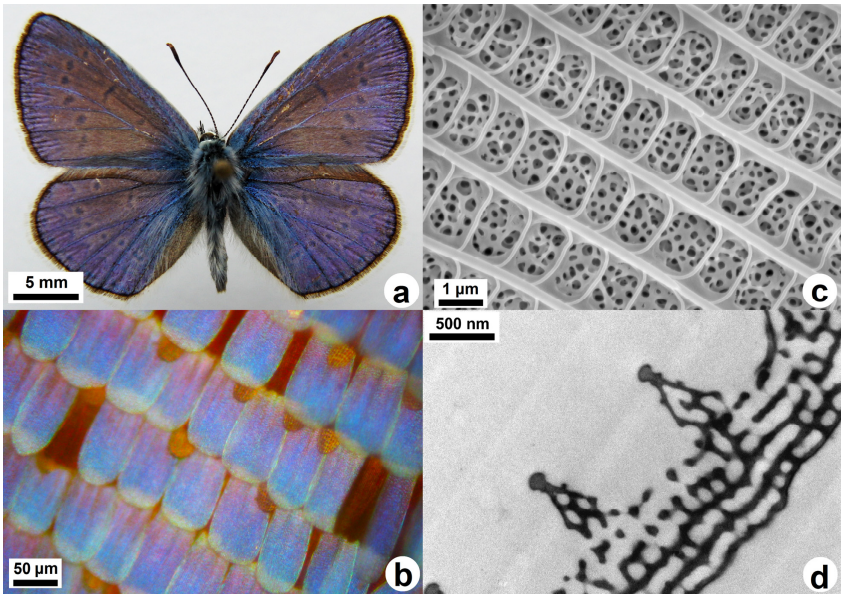

Fig. 1. (a) male *Polyommatus icarus* butterfly and (b) the blue dorsal wing scales of this species. (c) SEM and (d) TEM images of the chitin - air nanoarchitecture occurring in the blue wing scales.

In Fig. 2(a) the reflectance measurements on *P. icarus* can be seen during the vapor sensing experiment using a white diffuse standard (Avantes WS-1) as a reference. One can see how the reflectance spectra of the wing in synthetic air changes if the surrounding artificial air is replaced by the vapor mixtures of different concentrations. If disregarding the shift in the spectral position of the maximum, one may observe that the right hand side of the maximum does not move, while the left hand side, i.e., the blue – UV side exhibits the strongest alterations. Taking the blue wing in artificial air as a reference (Fig. 2(b)) the relative reflectance spectra showing the coloration changes during the experiment are obtained. It is clearly seen that the vapor mixtures in different concentrations cause the redshift and the slight desaturation of the wings which is the result of the capillary condensation of the vapors into the wing scale nanoarchitecture. As the vapor concentration is increased the amount of the condensate also increases, leading to more pronounced modifications of the spectrum. In our recent work temperature-dependent vapor sensing experiments [4] were carried out and we showed that the volatile vapors are present as liquids in the nanostructure. This is the likely explanation for the discrepancy between sensitivity and chemical selectivity to various vapors of butterfly wings found experimentally [1,10] and the lack of these according to calculations not taking into account the condensation of the volatiles in nanocavities [22].

#220109 - $15.00 USD Received 30 Jul 2014; revised 28 Aug 2014; accepted 28 Aug 2014; published 11 Sep 2014

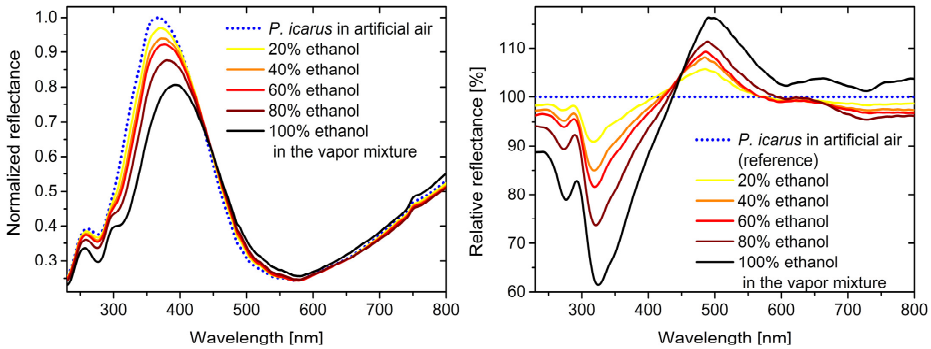

Fig. 2. (a) The alteration of the normalized reflectance spectrum of the *Polyommatus icarus* blue wing if the surrounding atmosphere is changed to artificial air – vapor mixtures in different concentrations. (b) Relative reflectance spectra of the same vapor sensing experiment when the *P. icarus* wing reflectance in artificial air flow was used as a reference.

In Fig. 3 the dynamic response can be seen during the vapor sensing experiment. Increasing concentrations of ethanol vapors were applied from 10% to 100% while the reflectance change signal in the 450 – 550 nm wavelength range were integrated according to the maxima in Fig. 2(b). It can be clearly seen that the signal is proportional with the vapor concentration [1,16] and rises in a few seconds after the vapor exposure (see the inset in Fig. 3). The characteristic response time and also the curve shape of the integrated reflectance change signal are similar for all applied vapors.

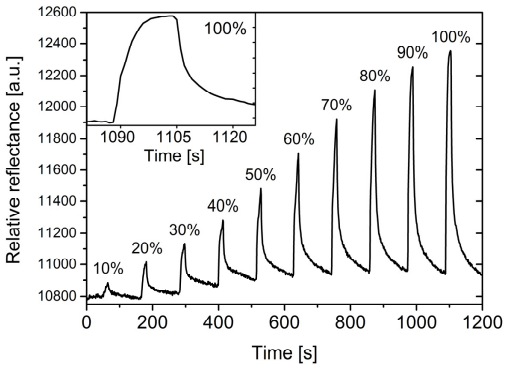

Fig. 3. The variation of the reflectance maximum integrated in the 450 – 550 nm wavelength range (see Fig. 2(b)) can be seen during the 20 minute long vapor sensing experiment using ethanol. The time-dependent signal rises and drops off in a few seconds (the magnified part of the curve can be seen in the inset) and it is proportional with the vapor concentration.

As we showed earlier the butterfly wing sensor is chemically selective [4,16], i.e. it provides characteristic reflectance signals to different vapors. To illustrate this, one can plot each reflectance spectra measured in a vapor environment using the tridimensional color space [11]. At this point we use reflectance curves corresponding to the highest signal at each concentration. In this way every sort of vapor in the plot will line up on a trajectory in the chromaticity diagram (Fig. 4(a)). Figure 4(a) was constructed using each individual spectrum measured in the concentration range from 10 to 100% (relative concentration) for each of the seven test vapors used and for artificial air, too. Every chromaticity point (with x, y, z chromaticity coordinates – as it can be seen in 'Materials and methods') in the 3D visual space of the butterflies [11] (Fig. 4(a)) corresponds to a reflectance spectrum measured at a certain concentration of one of the test vapors used. The location of each point is decided in a similar way as it is done for the usual human visual space (CIE 1931), with the difference that due to the fourth visual pigment of *P. icarus*, the visual space is not 2D – like for humans – but 3D.

#220109 - $15.00 USD Received 30 Jul 2014; revised 28 Aug 2014; accepted 28 Aug 2014; published 11 Sep 2014

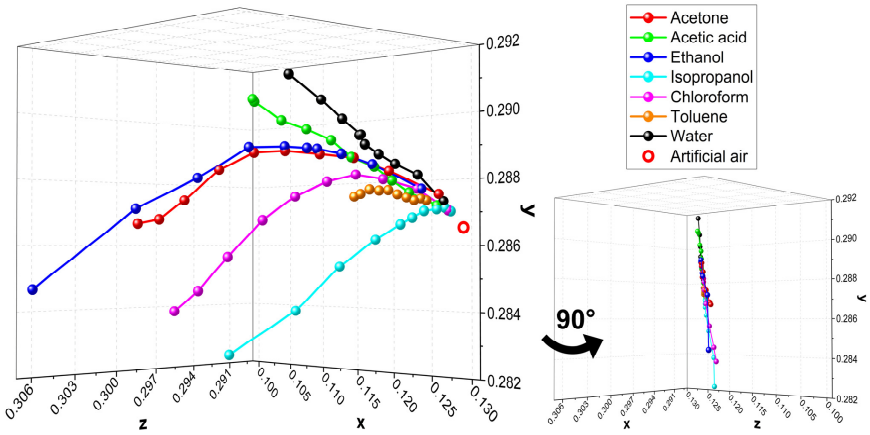

Fig. 4. (a) The result of the vapor sensing experiments in the 3D chromaticity diagram using 7 vapors at 10 concentrations. One can see the lower concentrations on the right and the higher concentrations on the left (the point corresponding to artificial air is labeled by red circle). (b) 90° rotated version of the 3D chromaticity diagram. One can see that the chromaticity points fit well onto a plane slightly different from the diagonal plain passing through the vertical edges facing the viewer.

Figure 4(a) was generated for the best visibility of the vapor sensing trajectories. While rotating it around the z axis, one can observe (Fig. 4(b)) that nearly all data points are clustered in a tilted plane. To keep the further investigations simple, a transformation was made to extract the 2D information of the vapor sensing data set by fitting a plane to the chromaticity values (x, y, z) in the 3D visual space and determining their local coordinates (x', y') in this 2D basis. These obtained local coordinates were plot as it can be seen in Fig. 6(a). It has to be pointed out that if the human visual space would be used – without taking into account the fourth visual pigment of the butterflies, than the spectral trajectories of Fig. 4(a) would look like in Fig. 5. In this case the chromaticity points of the seven vapors are clustered at the < 50% concentration range which shows that the minor color differences caused by the low vapor concentrations cannot be analyzed using the human visual space. This is similar to the unsatisfactory separation of the colors of the Polyommatine butterfly species in the human visual space [21].

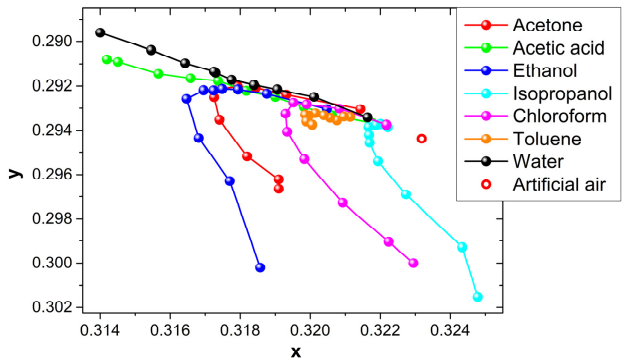

Fig. 5. The results of the vapor sensing experiment in the human, two-dimensional chromaticity diagram (CIE 1931). The chromaticity points of the low vapor concentration are clustered which shows the deficiency of the human visual space to discriminate low concentration vapors.

The butterfly chromaticity diagram results were obtained using as a hypothesis that the butterfly visual sensors have high selectivity at wavelength domains [13] where the small changes in wing coloration occur when mixing different vapors into the atmosphere surrounding the wing. As the butterfly eye has to be able to detect minor color differences (in

#220109 - $15.00 USD Received 30 Jul 2014; revised 28 Aug 2014; accepted 28 Aug 2014; published 11 Sep 2014

the blue range of the visible spectrum) for a successful mating, the fine tuning of the effect induced by the condensed vapors and its detector / analyzer should provide the highest possible selectivity for vapor sensing, too. As a verification and to analyze the obtained spectra, we applied PCA which is a pure mathematic evaluation method without any biological relation. In our case the input data were the reflectance signals of the *P. icarus* wing in Fig. 2(a) with 4.5 nm resolution, 69 rows in total, measured in 10% steps from 10% to 100% vapor concentration, which means 10 columns. The experiments were carried out for 7 vapors, so the input array contained 70 columns and 69 rows. The optimal number of PCs were two, which resulted 90.4% cumulative percentage of variance, which means that the second component retains over 90% of the original information. Using the same labeling as in Fig. 6(a), a trajectory is drawn for every vapor. The two graphs: one generated using the 3D butterfly visual space (Fig. 6(a)) and the other one produced by PCA (Fig. 6(b)), appear to be highly congruent.

The congruence of the curves obtained by PCA and using the visual space of the butterflies shows that both ways of evaluating the experimental data offer the same performance. This is an interesting finding as one of the methods - the PCA - is a complex man-made mathematical algorithm, while the butterfly eye and the associated visual space is the result of biologic evolution – developed together with the photonic nanoarchitecture responsible for the blue sexual signaling color, to enhance the success rate in mating encounters of butterflies. It is remarkable that these two very different ways of evaluating minor color differences give very similar results.

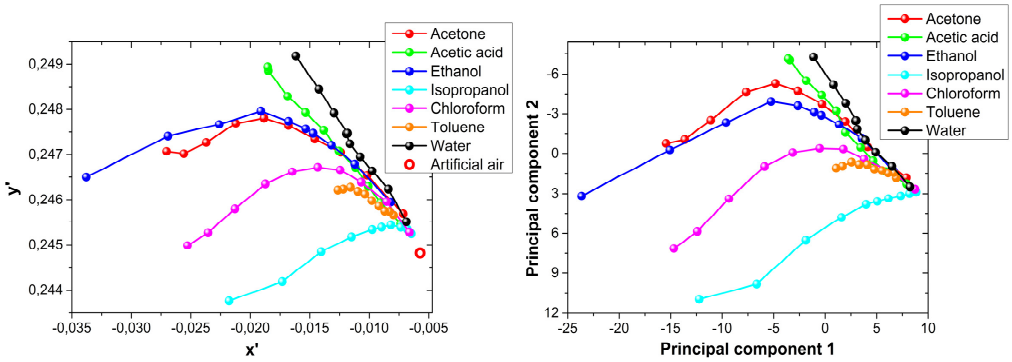

Fig. 6. (a) 2D transformed version of the 3D chromaticity diagram containing the results of the vapor sensing experiment. The red circle shows chromaticity point of the initial wing reflectance in artificial air from which the different vapor concentrations can be found right to left in ascending order. (b) The results of the PCA using the same vapor sensing data set.

Both in the chromaticity diagram and in the PCA results one can observe the good separation of the trajectories which represents the chemical selectivity, while the points representing different vapor concentrations follow each other (from right to left) in ascending order (of vapor concentrations) show the sensitivity of the sensor. It can be clearly seen that the good separation of the trajectories is based on their curvature at higher concentrations which suggests a reversible interaction between the chitin and the vapors. The reversibility was checked by the recovery of the original color after the vapor sensing experiments (see Fig. 3). To examine the hypothesis above, we investigated the origin of the color changing phenomenon caused by the vapors [16]. The main factor responsible for the change of the relative reflectance signal intensity is the penetration and condensation of vapors into the nanoarchitecture. This process is governed by capillary condensation [4] and through this the properties of the surface must have an important role in the evolution of the signal. We have shown recently that the conformal coverage of the butterfly wings using atomic layer deposition (ALD) with Al_2O_3 of a few nm thickness results in only slightly different wing reflectance signal compared to the uncoated wing [23] but it was shown earlier that the surface chemistry (e.g. wetting properties) of the butterfly wing scale can be tuned very

#220109 - $15.00 USD Received 30 Jul 2014; revised 28 Aug 2014; accepted 28 Aug 2014; published 11 Sep 2014

efficiently using ALD [24]. Therefore we used a 5 nm Al_2O_3 coated *P. icarus* wing as a sensor material to test to what extent the surface chemistry has an effect on the measured vapor sensing signal under the conditions given in the experimental section. The sample preparation details of the Al_2O_3 coated wings can be found in [23]. In this way we isolated the chitin nanoarchitecture from immediate interaction with the volatile vapors, the conformal coverage was checked by SEM investigation. We performed the same vapor sensing experiment as specified above. Compared to the results of the pristine wing case (Fig. 6(a)) the trajectories of vapors in the transformed 3D chromaticity diagram were altered as one can be seen in Fig. 7. There are major differences between the pristine and the ALD modified case: the coated sample has lower sensitivity and shows moderate selectivity. This is the result of the surface chemistry alteration inside the nanoarchitecture because the chitin was passivated by the conformal oxide layer. This is a clear indication that the selectivity and the sensitivity of butterfly wing sensors must have several components, it is not determined only by structural factors and refractive index contrast. As the characteristic structural elements of the photonic nanoarchitecture have dimensions in the order of 100 nm, the 5 nm ALD coating induces only minor changes both in dimensions and in refractive index contrast between the filled (chitin) and empty (air) components of the nanoarchitecture, still the response signals to the different vapors are strongly altered. It is reasonable to assume that these changes are associated with the surface chemistry of the nanoarchitecture, which may contribute by enhancing/retarding the nucleation of the first liquid droplets and after the condensation of the liquid the interaction of the solvent with chitin will differ if the 5 nm Al_2O_3 barrier is present, or not.

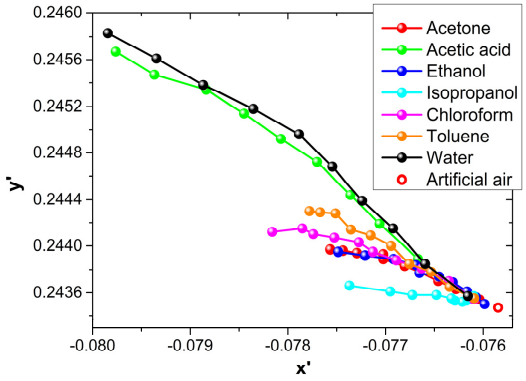

Fig. 7. 2D transformed chromaticity diagram results of the vapor sensing experiment using the butterfly wing modified with 5 nm conformal Al_2O_3 coating. The red circle shows chromaticity point of the initial wing reflectance in artificial air flow from which the different vapor concentrations can be found right to left in ascending order.

The 5 nm Al_2O_3 coating affects the surface chemistry of the sensor which lowers the sensitivity and selectivity but also changes the character of the optical response. While these changes are not desirable if sensor applications are targeted, the results clearly show that the surface modification of the photonic nanoarchitecture of biologic origin is a viable route to tune its response to the vapors present in the atmosphere surrounding it. Furthermore, it is worth to note that while in pristine state when increasing the concentration of the vapors from 10 to 100% the longest and the most curved trajectories were found for ethanol, chloroform and isopropanol, after the ALD coating these vapors show short trajectories with little curvature. Opposite, water and acetic acid (10% solution in water) in pristine state generated relatively short and almost straight trajectories, after the ALD coating these two vapors generated the longest trajectories with a certain degree of curvature.

To try to give a more quantitative comparison of the pristine and after ALD modified states, one can determine the distances between consecutive concentration steps in the chromaticity diagram for every vapor. Thus geometric distance will be calculated between the

#220109 - $15.00 USD Received 30 Jul 2014; revised 28 Aug 2014; accepted 28 Aug 2014; published 11 Sep 2014

consecutive points in Fig. 6(a) and Fig. 7 represented as column-diagrams. Each set of columns (pristine and modified) is normalized to 1, the total height of the highest column in the set – corresponding to the total variation of concentration from 0 to 100%. Different concentration steps are noted with different colors. The ideal sensor would show linear concentration dependence, so all color segments would have the same width. Figure 8 shows the column diagrams corresponding to the transformed 3D chromaticity diagram for the pristine (Fig. 6(a)) and ALD modified (5 nm Al_2O_3 deposition) (Fig. 7) wing. The pristine butterfly wing has more than five times higher response than the ALD modified wing.

Comparing the column diagrams of Fig. 8 one may remark that in both sets of experiments there are vapors which exhibit roughly equidistant steps as vapor concentration increases: acetone, acetic acid (10 vol% solution), chloroform and with slight deviations toluene and water, both for the pristine and for the modified wings. Two of the seven vapors: ethanol and isopropanol, on the other hand, exhibit a less regular increase of response and marked increase of the alteration as higher concentrations are attained, both for the pristine and the coated wings. Tentatively this is attributed to the penetration of these solvents into the volume of the chitin matrix, where they may produce swelling. At higher concentrations the capillary condensation is intensive – even the larger pores will be filled with liquid – in the pristine case the condensed vapors will interact easily with the biopolymer (chitin) [25]. After the ALD deposition the Al_2O_3 layer reduces the swelling changes (acting as barrier against the volume penetration of the liquid) therefore capillary condensation will be mainly responsible for the development of the signal. The nonlinearity of the trajectories may be attributed to the somewhat complex interplay of refractive index contrast modification (as the concentration of the vapors increases, progressively larger and larger nanopores will be filled with liquid) and with the onset of swelling that becomes dominant at higher concentration levels. The detailed examination of this interaction is beyond the scope of the present paper.

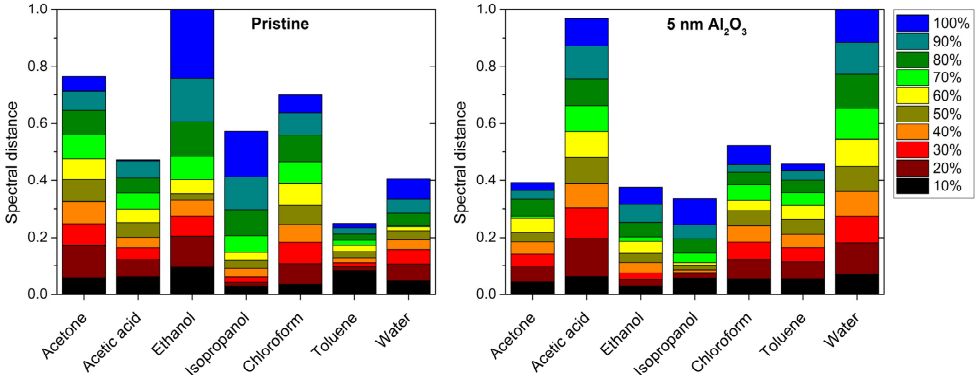

Fig. 8. Normalized column diagrams of the transformed chromaticity diagrams which show the distances between consecutive concentration steps for the seven vapors using (a) the pristine butterfly wing (b) and the ALD modified wing. The different colors show the different vapor concentrations. Note that the pristine wing has more than five times higher response. Both for the pristine and for the modified sensor the column height are normalized to the highest value for each sensor used.

Examining the transformed chromaticity diagram result of the pristine sensor (Fig. 6(a)) a difference can be observed between the lower and higher vapor concentrations. After a monotone section for < 50% concentration, at certain vapors the plot changes its inclination from upward to downward. After this, the distances of chromaticity points for consecutive concentration values may increase (ethanol, isopropanol). In the case of isopropanol this change occurs at much lower concentrations than for the other vapors. Water and acetic acid mixture remains close to linear over the whole concentration range. The change in the inclination of the curves for acetone, ethanol, chloroform, isopropanol and in the vicinity of 100% concentration, for toluene, too, is attributed to swelling effects. As the interaction of the different solvents with the chitin is expected to be different, it is justified to associate a certain

#220109 - $15.00 USD Received 30 Jul 2014; revised 28 Aug 2014; accepted 28 Aug 2014; published 11 Sep 2014

fraction of the chemical sensitivity to these different swellings. This interpretation is supported by the significant reduction of the chemical sensitivity after the ALD coating (Fig. 7).

As the band gap of a photonic crystal type structure is determined by the refractive index of the building materials, it is worth to try finding a correlation between the chromaticity diagram trajectories and the refractive index of the liquids. As discussed above, at higher concentrations there are swelling effects, but the lower range could be linear-fitted. Taking the slope of the linear fits for the low concentration part (< 50%) of the curves in Fig. 6(a) for every vapor, one can plot the relation of this slope and of the refractive index of the solvents in liquid state in Fig. 9. One can observe that there is a satisfactorily linear relationship between these two quantities. From Fig. 9 the isopropanol has been omitted as it exhibits a different behavior from the other vapors as can be seen in Fig. 6(a). As discussed above, this is associated with the swelling of the chitin nanoarchitecture. The acetic acid being a solution of 10% acetic acid in water has an estimated refractive index, where uncertainties may be responsible for the deviation from linearity. The other five (pure) solvents, with the exception of isopropanol, show a linear dependence between the index of refraction and the initial slope of the trajectories in the chromaticity diagram. This suggests that at lower concentrations the capillary condensation is the governing process and the swelling of the chitin nanoarchitecture becomes dominant only at higher concentrations, because of the high amount of volatile liquid condensed into the nanoarchitecture exhibiting a stronger interaction with chitin. This is consistent with the results of the simulations [22] and it can be clearly observed in the chromaticity diagram after the ALD process (Fig. 7): the curvatures disappear from the vapor sensing trajectories when the Al_2O_3 coating is applied because the isolation of the chitin from the condensed volatiles does reduce significantly the swelling of the chitin nanoarchitecture. Therefore, the capillary condensation, i.e., the refractive index contrast change of the nanoarchitecture is the dominant process which affects the color change of the butterfly wing.

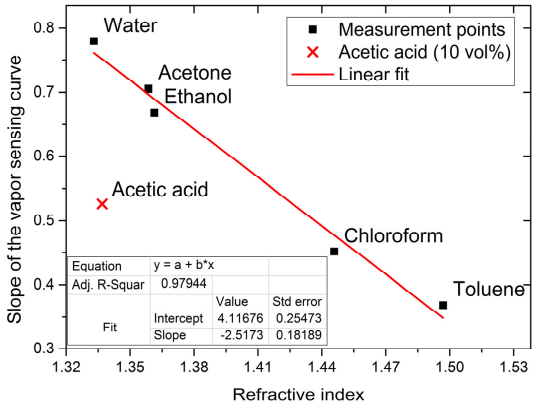

Fig. 9. The slopes of the linear-fitted segments of the vapor sensing trajectories are proportional with the refractive indices of the different volatiles. Acetic acid (10 vol% water mixture) was left out from the linear fit.

It is worth to be pointed out that chitosan prepared from chitin, and chitosan based polymer membranes can be used very efficiently for the separation of isopropanol - water vapor mixtures through pervaporation [25]. This suggests that the chitin based structures may have a particular affinity towards isopropanol, and this could be the reason for which the swelling is the dominant process in the case of isopropanol vapors already at low concentrations. Photonic nanoarchitectures occurring in the wing scales are supposed to show similar strong interaction with isopropanol, which will affect the color changing characteristics, therefore the vapor sensing properties of the butterfly wing. In this sense the

#220109 - $15.00 USD Received 30 Jul 2014; revised 28 Aug 2014; accepted 28 Aug 2014; published 11 Sep 2014

effect of isopropanol cannot be interpreted completely with the capillary condensation or geometric change of the structure thus it was not analyzed this way.

4. Conclusions

We investigated the chemically selective vapor sensing properties of the photonic nanoarchitectures in the Common Blue (*Polyommatus icarus*) wing scales using the spectral shift of the reflectance maximum of the blue dorsal wing side. The spectra were analyzed using the three-dimensional chromaticity diagram [11] based on the color vision of the Polyommatine butterflies, a fully "biologic" approach. Control evaluation was carried out using PCA – a fully "mathematical" approach – an almost perfect match of the two results was observed. This clearly shows that the 3D chromaticity diagram is very suitable for the analysis of the vapor sensing data sets: it can be used very efficiently for the characterization of the spectral changes produced by the different vapors which results the good chemical selectivity of the sensor. Good separation of substance specific trajectories was found, with both methods, using seven test volatiles to show the sensitive and selective vapor sensing behavior of the butterfly wings. It is remarkable that the two very different ways of analyzing the same experimental data – the biologic one and the mathematical one – produced almost coincident results. In a somewhat surprising way this shows that in the wavelength region where the scales of the males generate structural color the vision of the *P. icarus* butterflies equals the selectivity of a sophisticated mathematical algorithm.

We investigated the interaction between the chitin nanoarchitecture and the volatile vapors. A 5 nm Al_2O_3 coated *P. icarus* wing was used in the vapor sensing experiment with the seven volatiles. Reduced sensitivity and selectivity were observed when the chitin was isolated from the vapors which suggest a reversible chemical interaction (swelling) between the sensor material and the volatiles in the pristine wings. This interaction is vapor-specific which in part is the source of the chemical selectivity. The detailed analysis showed that at lower concentrations the dominant process is the capillary condensation of the vapors into the nanoarchitecture, while at higher concentrations the chitin swelling becomes dominant for acetone, ethanol, chloroform and toluene. For isopropanol the swelling is important already in the low concentration range.

The possibility to tune the response of the photonic nanoarchitectures by the modification of their surface by well-established materials science methods may offer a wide range of possibilities to sensitize / desensitize the sensors for certain volatiles and to produce sensor arrays, which can be very useful in "fingerprinting" the substances to be recognized, which can enhance significantly the selectivity of the array.

Acknowledgments

This work was supported by the Hungarian OTKA PD 83483 and OTKA K 111741.

#220109 - $15.00 USD Received 30 Jul 2014; revised 28 Aug 2014; accepted 28 Aug 2014; published 11 Sep 2014